One million satellites in the sky: Light contamination on space telescopes

Alejandro Borlaff

a.s.borlaff@nasa.gov

NASA Ames Research Center https://orcid.org/0000-0003-3249-4431

Pamela Marcum

NASA Ames Research Center

Steve Howell

NASA

Physical Sciences - Article

Keywords: Space telescopes (1547), Artificial satellites (68), Light pollution (2318), Hubble Space Telescope (761), Space observatories (1543), Interdisciplinary astronomy(804)

Posted Date: April 18th, 2025

DOI: https://doi.org/10.21203/rs.3.rs-6414845/v1

Additional Declarations: There is **NO** Competing Interest.

Version of Record: A version of this preprint was published at Nature on December 3rd, 2025. See the published version at https://doi.org/10.1038/s41586-025-09759-5.

One million satellites in the sky: Light contamination on space telescopes*

Alejandro S. Borlaff[1*], Pamela M. Marcum[1] and Steve B. Howell[1]

[1*]NASA Ames Research Center, Space Science and Astrobiology Division, N245, Moffett Field, 94035, CA, USA.

*Corresponding author(s). E-mail(s): a.s.borlaff@nasa.gov;
Contributing authors: pamela.m.marcum@nasa.gov;
steve.b.howell@nasa.gov;

Abstract

Rapidly growing satellite mega-constellations have raised strong concerns among the scientific community. Reflections from satellites are visible to the human eye and extremely bright for professional telescopes. These trails already affect astronomical observations across the complete electromagnetic spectrum, with a noticeable cost for operations and mitigation efforts. Despite the common misconception, satellite trails affect not only ground-based observatories, but also space observatories, like *Hubble*. However, the current number of satellites is only a fraction (<10%) of those to be launched in the next decade. Here we show a forecast of the satellite trail contamination levels for a series of international low earth orbit telescopes, based on the proposed telecommunication industry constellations. Our results show that if these constellations are completed, one fourth of *Hubble*'s images will be contaminated, while the space telescopes SPHEREx, ARRAKIHS, and *Xuntian* will have **94%** of their exposures affected, with $\mathbf{5.9^{+0.6}_{-0.6}}$, $\mathbf{32^{+17}_{-13}}$ and $\mathbf{86^{+20}_{-19}}$ trails per exposure respectively, with an average surface brightness of $\boldsymbol{\mu = 18 \pm 2}$ mag arcsec$^{\mathbf{-2}}$. Our results demonstrate that light contamination is a growing threat for space-telescope operations. We propose a series of mitigation measures to minimize their impact, allowing researchers to predict, model, and correct unwanted satellite light pollution from science observations.

Keywords: Space telescopes (1547), Artificial satellites (68), Light pollution (2318), Hubble Space Telescope (761), Space observatories (1543), Interdisciplinary astronomy(804)

*Submitted on April, 9th, 2025

1 Introduction

Until 2019, the largest constellation of artificial satellites was the *Iridium* system, with 75 spacecraft in Low Earth Orbit (LEO) at altitudes between $h \sim 160 - 1600$ km. Radio-emission in the 1621-1628 MHz band by *Iridium* satellites was one of the first sources of electromagnetic pollution from space to be addressed by the calibration pipelines[1] of ground-based observatories [1]. Over the past few years, the number of satellites has increased to approximately ∼15,000. Due to the reduction of the cost-per-kilogram of launching payloads to LEO, the number of artificial satellites has grown exponentially since 2020. Over this era, the proposals of telecommunication satellites to the US Federal Communications Commission (FCC) and the International Telecommunication Union (ITU)[2] have increased by two orders of magnitude [2]. Launches are expected to be even more accessible in the future, as the advent of next generation superheavy launchers (SLS, *New Glenn*, *Starship*, *Long March 9*) will likely reduce the launch cost and increase the capability to deploy more satellites and to even higher orbits. At the current rate, Earth would be orbited by one million artificial satellites by the end of the 2040 decade [2].

Early observations of the first *Starlink* satellites in 2019 revealed that reflected light from the solar panels was easily visible to the unaided eye, interfering with ground-based observatories at all wavelength ranges [3–5]. As their relative position in the sky changes, they leave a trace of light in the exposures of astronomical images, called satellite trails. Satellite trails contaminate the targets of science interest, generating light gradients (scattered light), and increasing the photon-noise. For new generation ground-based telescopes such as the *Vera C. Rubin* Observatory [6], it is estimated that 20% of the midnight images will present satellite trails, and between 30% to 80% of all exposures obtained at the beginning and end of the night will be affected [7, 8].

Since LEO satellites are detected through reflected solar light, they are mostly visible to the unaided eye at twilight during sunset and sunrise. Most mitigation efforts[3] have been focused on making the satellites sufficiently dim so that they are not detectable by the human eye ($m_{\rm vis} \sim 6-7$ mag). The typical apparent magnitude of the first generation *Starlink* satellites was $m_G = 5.1 \pm 1.1$ Gaia G magnitudes [9]. Dark coatings and optical blocking systems have proven to be inefficient in avoiding the presence of satellite trails [8] in astronomical imagery data, with only a mild decrease of the optical magnitude of the satellites [from 4.6 to 5.9 mag, in the case of VisorSat, and 7.3 in the case of DarkSat 9, 10], reducing the visual impact for unaided-eye observers, but remaining extremely bright for astronomical observatories. In fact, newly launched Direct-To-Cell (DTC) satellites present much larger solar panels (125 m^2 vs. 26 m^2) and are much brighter than regular internet satellites [up to $m_{opt} \sim 0-1$ mag, compared to the original 4 – 6 mag, 11]. Super-bright satellites such as Blue Walker 3 are comparable to the magnitude of the brightest stars in the sky [12].

[1] NRAO/VLA - Calibration in the Presence of Iridium: https://www.vla.nrao.edu/astro/calib/manual/irid-cal.html

[2] International Telecommunication Union: https://www.itu.int/ITU-R/space/asreceived/Publication/AsReceived

[3] Starlink presentation on AAS 2021: https://aas.org/sites/default/files/2020-06/SpaceX%20for%20SIA%20AAS%20Astronomy%20Webinar%205.26.20.pdf

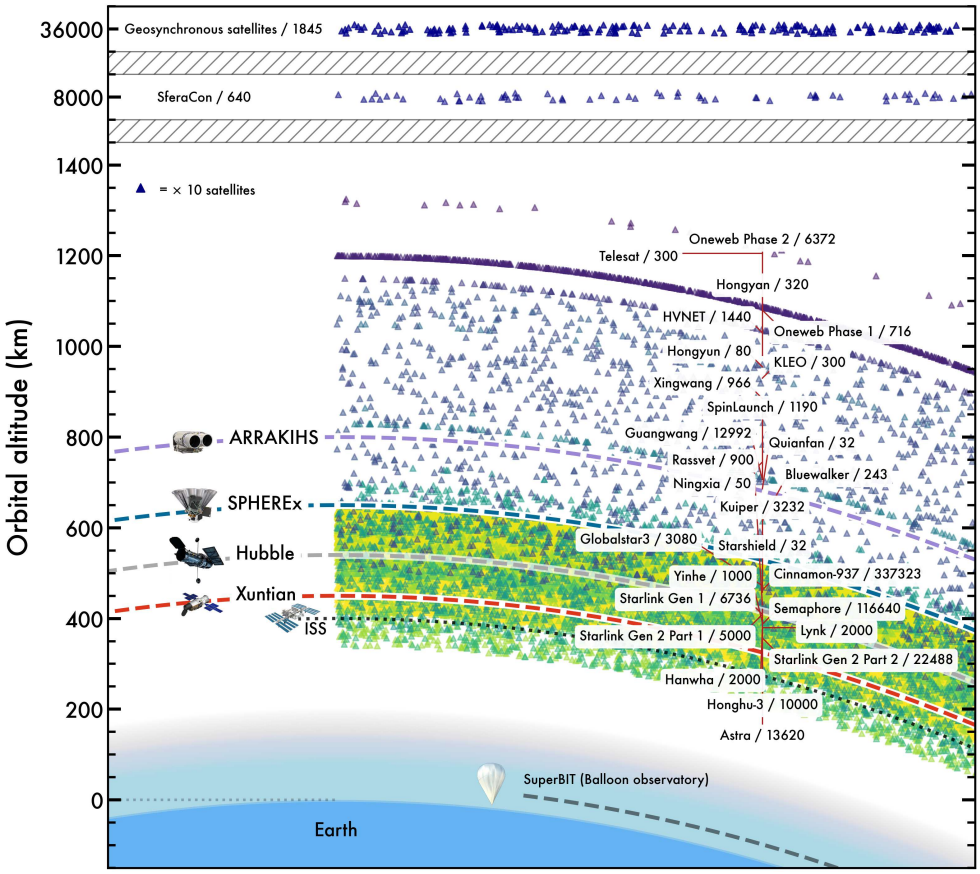

Fig. 1 Structure of proposed satellite telecommunication constellations in Low Earth Orbit as registered in March 11, 2025. The altitude of satellites is compared to the orbits of *Hubble* Space Telescope, *Xuntian* Space Telescope (CSST), SPHEREx, and proposed ARRAKIHS mission (see Table 1). Constellation labels show the number of proposed satellites. Each symbol represents 10 satellites.

Mitigation strategies have included pausing ground-based telescope operations during the twilight and sunrise hours, when the satellites with lowest-altitude orbits ($h < 600$ km) are most visible [13]. While utilizing this technique avoids many of the brightest satellite trails with orbit altitudes below $h \sim 600$ km, some critical scientific programs such as discovery surveys for unknown hazardous Earth orbit-crossing asteroids can only be conducted through twilight and sunrise observations, exactly when the satellite trails are most common [14]. Satellites at higher altitudes may pose an even greater challenge as they can be visible for longer periods or even continuously, contaminating images obtained even at midnight. With prospects of hundreds of thousands of satellites already proposed at altitudes between 340 – 8000 km (Table 1), the fraction of uncontaminated night sky is at risk of becoming too small for practical science operations.

While much attention has been directed at the future of ground-based astronomy, the impact on space telescopes by a crowded near-Earth space environment has been poorly explored. This manuscript is focused on the prediction of the image degradation by satellite trails in present and near-future LEO space telescopes. The observations of active space telescopes are already being contaminated by artificial satellite trails. Recent works [15] demonstrate that 4.3% of the images obtained by *Hubble* between 2018 and 2021 already present artificial satellite trails. Considering that the proposed number of satellites is two orders of magnitude higher than current, the fraction of impacted images will increase very soon. Table 1 gives a summary of the properties of all planned and present satellite mega-constellations, together with the orbits of several observatories. Most satellite layers are planned between 500 to 700 km, with extended constellations up to 8000 km (see Fig. 1). As a consequence, LEO observatories and every balloon-borne telescope will be affected by these satellites.

To forecast the frequency of satellite trails in LEO space telescopes, this paper simulates the observations of four different platforms: 1) *Hubble* Space Telescope, 2) the Spectro-Photometer for the History of the Universe, Epoch of Reionization, and Ices Explorer [SPHEREx, 16], 3) *Xuntian* Space Telescope [also known as Chinese Space Station Telescope, launch planned for 2026, 17, 18], and 4) ARRAKIHS Space Telescope [ESA F-class proposed mission, to be launched no earlier than 2030, 19, 20]. The specifications considered for each telescope in terms of orbital altitude, inclination, wavelength range, field of view, and spatial resolution are detailed in Table 2. Simultaneously, we simulate a series of constellations following the announced orbital configurations (altitude, number of shells, planes, and satellites per plane) to the FCC and the ITU up to date (March 2025), with increasing numbers up to one million satellites, aiming to estimate the number of trails detected by the telescopes per average exposure. The simulated telescope observations take into account realistic survey plan constraints (Earth avoidance angle, exposure time, maximum zenith angle) and configuration of the telescope (orbit, field of view). The predicted number of satellite trails observed per exposure and their surface brightness on each telescope is presented in Sec. 2. The methodology is further described in Sec. 3. We discuss their impact in science operations and potential mitigation strategies in Sec. 4.

2 Results

2.1 Satellite trail frequency

Our simulated images (Fig. 2) underscore the dramatic rise in satellite trail contamination with increasing number of Low Earth Orbit satellites (see Fig. 3). If the population of artificial satellites surpasses 100,000 (1/6 of the proposed number of satellites to the ITU and FCC), SPHEREx would observe at approximately 2.8 ± 0.4 Sun-illuminated satellite trails on an average exposure ($88 \pm 5\%$ of the exposures would contain at least one trail). For ARRAKIHS and *Xuntian*, the predicted number of trails is much higher, close to 7 ± 3 and 16 ± 4 average trails per exposure. If the planned constellations are completed ($N_{\rm sat} \sim 560,000$), the average number of trails would rise to $5.9^{+0.6}_{-0.6}$, 33^{+17}_{-13}, and 86^{+20}_{-19} for SPHEREx, ARRAKIHS, and *Xuntian* respectively

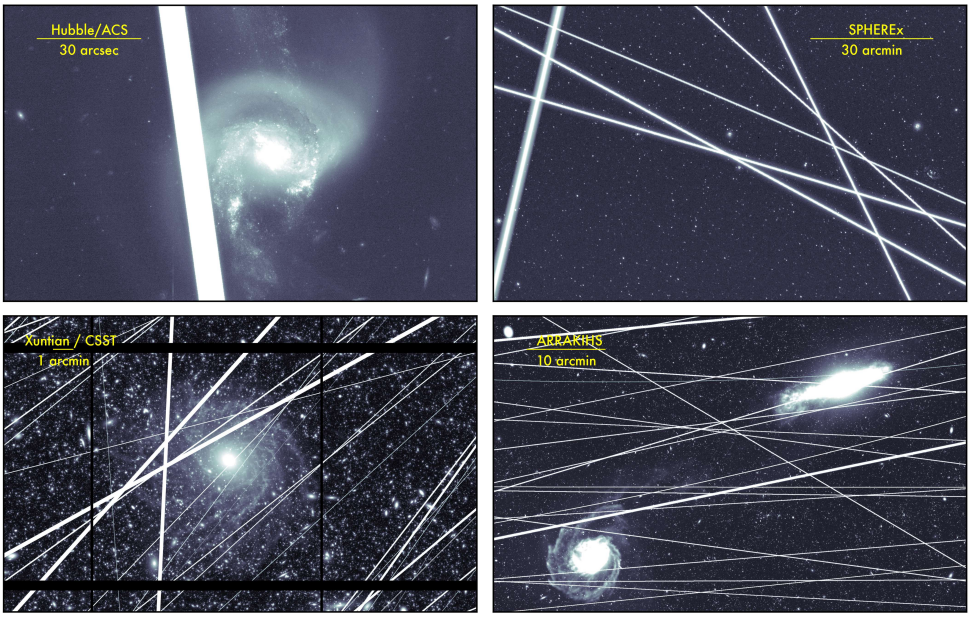

Fig. 2 Simulated exposures for *Hubble*, SPHEREx, *Xuntian*, and ARRAKIHS (see labels) space observatories, showing satellite trails contamination. The satellite trails were generated by simulating the orbits of $N = 1,000,000$ satellites using the orbital and physical parameters of the announced constellations to be operational by 2040 (see Fig. 3). Background galaxies based on [21, 22].

(94 ± 3% of the exposures affected). At this level, one every four *Hubble* simulated images show satellite trail contamination.

Relative to ARRAKIHS or *Xuntian*, SPHEREx's substantially larger FOV (39.5 deg^2 vs. 1.2–1.4 deg^2) increases the probability of a satellite being detected by the telescope. However, its strict pointing constraints and higher altitude compared to *Xuntian* (650 km vs. 450 km) compensate the risk. In particular, the strict maximum zenith angle requirement (35 deg) excludes the regions of the sky closer to the limb of the Earth where a higher number of satellites are visible per square degree. *Xuntian* presents the higher contamination levels of all the considered telescopes, due to its lower orbit altitude. In the case of ARRAKIHS, despite being in a higher orbit (800 km) and having a relatively lower field of view than SPHEREx (1.4 deg^2), the observing plan requires long exposure times (600 s), potentially reaching orientations closer to the limb of the Earth than SPHEREx, thus increasing the probability of a satellite crossing the detector[4]. This result indicates that stricter observational requirements can reduce the number of trails in ARRAKIHS and *Xuntian* at the expense of a shorter observational time per orbit, and a reduced observable area.

Under current conditions ($N_{\rm sat} \sim 15,000$) we predict that 81.3±1.8% of SPHEREx observations will present at least one satellite trail, when measured over an entire

[4] ARRAKIHS and *Xuntian* are still in development phase, so their operational constraints could adapt or change.

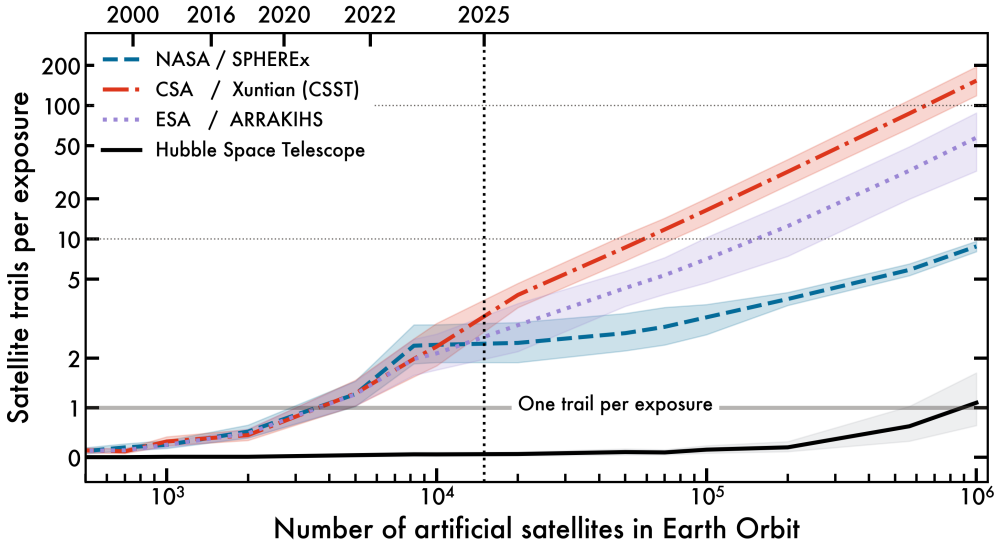

Fig. 3 Mean number of satellite trails per exposure as a function of the population of artificial satellites in Earth orbit (lower $x-$axis) and epoch (upper $x-$axis). *Blue:* SPHEREx, *Red: Xuntian*, *Purple:* ARRAKIHS. *Black: Hubble* Space Telescope. Contours represent the 95% confidence levels for the mean number of trails. *Horizontal solid line:* One trail per exposure critical contamination level. *Vertical dotted line:* Current number of active and inactive satellites in orbit (15,000 as of March 2025).

year. We validated the methodology by comparing satellite trail detection in recent *Hubble* Space Telescope data to predictions from simulations based on the satellite population in October 2021 (5589 satellites of large sizes > 1 m^2). Our simulations predict $4.2 \pm 0.7\%$ of recent images should present at least one satellite trail, a value consistent with the rate of $4.3 \pm 0.4\%$ observed in *Hubble* ACS/WFC images acquired between 2018-2021. *Hubble* Space Telescope's substantially narrower field of view (2×2 arcmin) decreases observed trail frequency to 10 times lower than that of SPHEREx. Only after the population of artificial satellites has exceeded 700,000 would *Hubble* display, on average, one sun-illuminated satellite trail in every exposure. At population levels of 1,000,000 satellites, *Hubble* would observe an average of $1.1^{+0.6}_{-0.5}$ satellites per exposure ($28.1 \pm 8.8\%$ of the images would show one trail or more). For comparison, SPHEREx, ARRAKIHS, and *Xuntian* will observe $8.8^{+0.8}_{-0.8}$, 57^{+29}_{-24}, and 150^{+41}_{-34} satellite trails per average exposure, respectively.

2.2 Satellite trail brightness

A satellite crossing the field of view of a telescope does not guarantee that the satellite trail will be visible in the imagery data. The surface brightness magnitude of a satellite trail depends on several factors, including the apparent speed (the faster a satellite crosses the detector, the dimmer the trail will be), source of illumination (Sun, Moon),

satellite area (larger satellites are brighter), distance from observer to the satellite, and the attitude of the satellite surfaces with respect to the illumination source and the observer.

Due to the limited availability of information specifying shape and optical properties for commercial satellites, a precise prediction of the brightness of satellite trails is not currently possible. We discuss potential mitigation measures in Sec. 4. However, we can provide order of magnitude estimations of the peak surface brightness of the satellite trails based on the current observations of satellite mega-constellations and the results from the simulations presented above. The methodology to quantify the satellite trail surface brightness is detailed in Sec. 3.3.

Our simulations predict a surface brightness for satellites trails between $\mu = 16$ to $\mu = 22$ mag arcsec^{-2}. In particular, *Hubble* and *Xuntian* would image the brightest trails, $\mu = 16.5 \pm 1.1$ mag arcsec^{-2} and $\mu = 16.7 \pm 1.2$ mag arcsec^{-2} respectively, followed by ARRAKIHS ($\mu = 17.3 \pm 1.3$ mag arcsec^{-2}), and SPHEREx ($\mu = 18.2 \pm 4.9$ mag arcsec^{-2}). The predicted difference in surface brightness is mainly caused by the spatial resolution of the telescopes: higher resolution leads to enhanced flux concentration, which results in increased surface brightness. As a verification, we measure the surface brightness of the only confirmed *Starlink* satellite trail observed by *Hubble*, in November 2nd, 2020 (*Starlink* 1619, `iedk12aoq`, WFC3/UVIS F350LP, PID: 16183, Porter, S.). The satellite trail has an approximate width of 7.9 arcsec (200 pixels) and a surface brightness of $\mu = 18.0 \pm 0.1$ mag arcsec^{-2}, compatible with the predicted *Hubble* trail brightness distribution in our simulations. A relatively dimmer-than-average observed brightness is expected since the trail in the *Hubble* exposure `iedk12aoq` was spatially resolved (trail width of 90 ± 20 pixels), spreading the flux over a larger number of pixels, and that *Starlink* 1619 belongs to the first version of the constellation with a much smaller area (25 m^2) than their newer version (125 m^2).

Finally, we consider the case of satellites only illuminated by the full Moon ($m_{\odot,V} = -12.74$). In that case the predicted trail surface brightness for the four telescopes is well below detectability levels for single exposures: $\mu = 30.3 \pm 1.1$ mag arcsec^{-2} for *Hubble* and *Xuntian*, and $\mu = 31.8 \pm 1.1$ and $\mu = 33.2 \pm 4.9$ mag arcsec^{-2} for ARRAKIHS and SPHEREx, respectively. Only sun-illuminated satellites were detectable and considered in our simulations (Fig. 3 and Sec. 2.1).

3 Methodology

3.1 Space telescopes orbit and attitude simulation

The key objective of this work is the prediction of the number of satellite trails in future and present space telescopes in different configurations, represented by *Hubble* Space Telescope, the terminator-aligned sun-synchronous orbit SPHEREx space telescope (700 km), *Xuntian* Space Telescope (450 km), and the proposed ESA mission ARRAKIHS ($\sim$ 800 km). The main properties of the four telescopes are summarized in Table 2. We note that *Xuntian* and ARRAKIHS are missions still in development, and their configurations might change before launch. In particular, ARRAKIHS proposed orbit ranges from 650 to 800 km [19]. Since satellite contamination becomes less

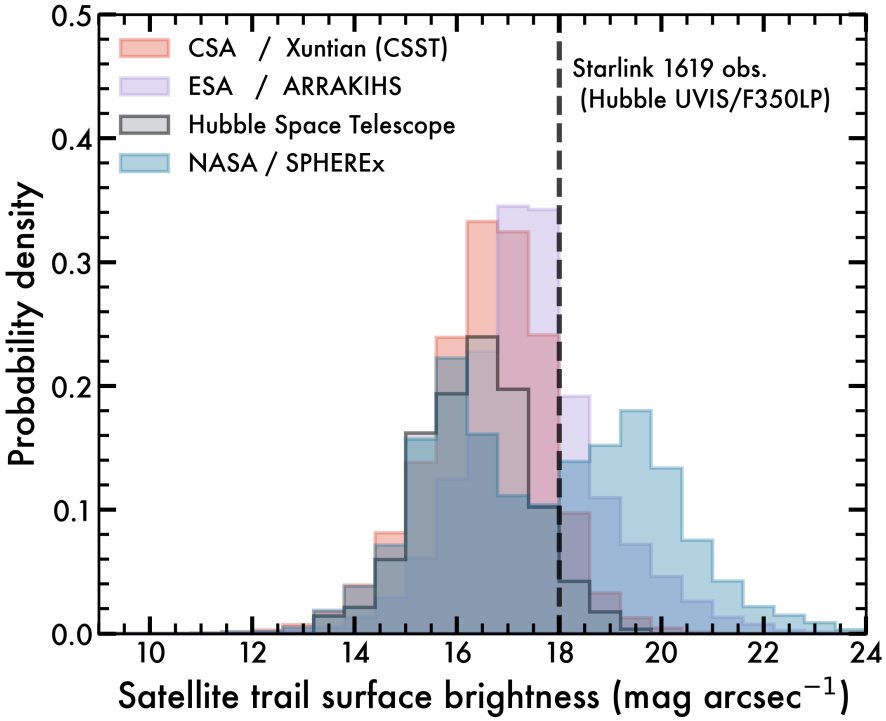

Fig. 4 Histogram of satellite trail surface brightness, separated per observatory. *Blue:* SPHEREx, *Red: Xuntian*, *Black: Hubble* Space Telescope. *Vertical dashed line:* Observed surface brightness of satellite trails in *Hubble* Space Telescope, estimated from the WFC3/UVIS F350LP observation of Starlink 1619. *Hubble* observation PI: S. Porter (MAST PID: 16183). Satellite ID by J. McDowell.

frequent at higher orbits, we chose a best-case scenario with a 800 km orbit for the calculations.

The satellite trail simulation process is schematized in Fig. 5. For each observatory, we assume a survey plan which consists of a series of pointings (right ascension and declination) taking place at an associated epoch (epoch at exposure start $t_{\rm start}$ and exposure end $t_{\rm end}$) with a certain exposure time ($t_{\rm exp} = t_{\rm end} - t_{\rm start}$). The available regions on the sky depend on the telescope orbit (as defined by the Two Line Element, or TLE) and epoch (i.e., a telescope cannot observe a region blocked by Earth), and specific survey constraints (i.e., Sun avoidance, Earth-limb, and maximum zenith angles) for each telescope, summarized below. We assume a fixed orbit for SPHEREx and *Xuntian* telescopes (see Supplementary information 4.1). For *Hubble* simulations, we randomly select archival exposures (right ascension, declination, $t_{\rm start}$, $t_{\rm exp}$) obtained with the wide field channel of the Advanced Camera for Surveys (ACS)

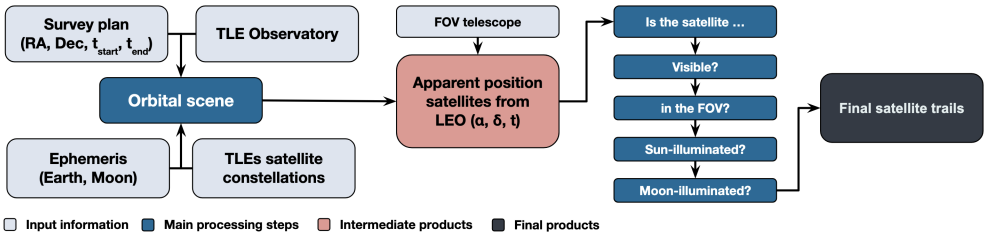

Fig. 5 Satellite trail simulation methodology flowchart. Left to right: 1) Orbital scene, based on the survey plan, Earth and Moon ephemeris, telescope (observer) and artificial satellite orbits. 2) Estimated sky position of the satellites along the simulated exposure. 3) Filtering satellite trails that cross the field of view, and are illuminated by the Sun or the Moon. 4) Final record of satellite trail contamination on each exposure.

during 2023-2024, assuming the closest orbit on time from its recorded history[5]. The typical exposure time was $t_{\rm exp} = 540^{-200}_{+530}$ s.

To simulate the survey plan, orbital position, and attitude of the SPHEREx, *Xuntian*, and ARRAKIHS space telescopes, we choose random locations in the sky that are accessible with the adopted constraints of each telescope. For SPHEREx, we assume a maximum zenital angle of 35°, 91° Solar-avoidance angle during the whole exposure, and a exposure time of 112.5 s on a $h = 650$ km terminator-aligned sun-synchronous orbit [23]. Similarly, we choose a $h = 800$ km terminator-aligned sun-synchronous orbit ARRAKIHS, with a fixed exposure time of 600 s [19], and 7.6° Earth-limb angle (as in *Hubble*). Finally, *Xuntian* was assigned the same orbit as the Tiangong Space Station (LEO, $h = 450$ km, $i = 41.47°$), 55° Solar-avoidance angle, 7.6° Earth-limb angle during the whole exposure, and a random exposure time following the same distribution as the *Hubble* observational record.

3.2 Satellite constellations orbit

The orbital parameters for the satellite constellations were generated[6] using `Planet489` public database[7] of the orbital altitude, number of shells, number of orbital planes, and satellites per plane on each FCC/ITU registered satellite constellation. In addition to the simulated satellite constellations based on the orbits described on Table 1, we include a baseline of existing satellites, which include every already existing Earth artificial satellite, removing 1) those classified as part of constellations (to avoid duplications), 2) cubesats, 3) debris, or 4) objects known to be too small to be observed (i.e., Westford Needles). To analyze the effect of an increasing population of artificial satellite constellations, we randomly choose a varying number of satellites, starting from a baseline population ($N \sim 100$) up to one million satellites. The simulated satellites are chosen randomly from the pool described before for each simulation, ensuring that we sample the potential variability of scenarios.

[5] Celestrak: https://celestrak.org/
[6] `Bulk TLE Generator`: https://tle-generator.starlitter.info/
[7] `Planet489`: https://planet4589.org/index.html

Based on the orbital parameters and telescope survey plans, the cartesian geocentric position ($\overline{x}_t = (x,\ y,\ z,\ t)$) of the telescope (observer) during the exposure is calculated. In parallel, the coordinates of the satellite constellation are estimated ($\overline{x}_s$). Then, the apparent location on the sky (right ascension, declination) of the Earth, Sun, Moon, and the artificial satellite constellation are computed within the local reference frame of the telescope. The location and extension of the Earth and the Moon are determined using their predicted ephemeris and physical properties, while the apparent location of the artificial satellites are simulated as a function of time by propagating their orbits. Thanks to the described approach, we can determine which satellites are visible (not behind the Earth), illuminated by the Sun and/or the Moon, and/or inside the field of view of each telescope. The code is based on `Python/Skyfield` [24]. The final product is a database (satellite trails) of the location of each satellite that crosses the field of view, including their brightness, angular speed, illumination by the Sun or the Moon, the distance to the observer, and the location in the sky as a function of time.

3.3 Satellite trail brightness

The surface brightness of satellite trails depends on multiple factors, including: 1) the brightness of the light source, 2) the Bidirectional Reflectance Distribution Function [BRDF; 25] of the satellite, and 3) the orientation of the reflecting surfaces to the observer. For order of magnitude estimations, we implement some simplifying assumptions.

A satellite located at a distance $d_{\rm sat}$ from a space telescope with a mirror diameter $D_{\rm mir}$ crossing the FOV leaves a trail with a width $\theta_{\rm sat}$ defined by [26]:

$$\theta^2_{\rm sat} = \frac{4R^2_{\rm sat} + D^2_{\rm mir}}{d^2_{\rm sat}} + \sigma^2. \tag{1}$$

where σ represents the minimum resolution element (or seeing in the case of a ground-based telescope), and $R_{\rm sat}$ is the equivalent radius[8] of the cross-sectional area of a satellite, assuming a random orientation between 0° to 180° with respect to the observer. The area of the extended solar panels in new generation satellites can range from 1 $\rm m^2$ up to 125 $\rm m^2$ [11]. In this work, we assume a uniform distribution between these two extreme values.

The apparent magnitude ($m_{\rm sat}$) of the satellite can be approximated as [27]:

$$m_{\rm sat} = m_{\odot} + 2.5\log_{10}\left(\frac{\rm d^2_{sat}}{pR^2_{\rm sat}}\right) \tag{2}$$

where p is the geometric albedo of the satellite and $R_{\rm sat}$ is the equivalent radius of the satellite cross-section. Assuming a representative example, for Starlink satellites, $p = 0.25$ [7]. We adopt $m_{\odot,V} = -26.77$ for the magnitude of the Sun, and $m_{\odot,V} = -12.74$ for the magnitude of the Moon at a reference wavelength of $\lambda_{\rm ref} = 0.55\,\mu$m. The peak surface brightness magnitude of the satellite trail $\mu_{\rm sat}$ (in mag $\rm arcsec^{-2}$)

[8] Equivalent radius is defined as the radius of a circle with the same area.

depends on the apparent magnitude of the satellite $m_{\rm app}$ (mag), its focal plane velocity $\omega_{\rm sat}$ (arcsec s^{-1}), and the exposure time $t_{\rm exp}$ (s):

$$\mu_{\rm sat} = m_{\rm sat} - 2.5\log_{10}\left(\frac{4}{\pi\theta_{\rm sat}\omega_{\rm sat}t_{\rm exp}}\right). \quad (3)$$

4 Discussion

Mitigation is only possible after careful quantification. Our results show that astronomical images from current and new generation space telescopes will be contaminated by light reflected from telecommunication satellite mega-constellations in low Earth orbit. If all proposed satellite constellations are completed, we forecast that 94% of the exposures of SPHEREx, ARRAKIHS, and *Xuntian* will present at least one Sun-illuminated satellite trail, as well as one forth of all *Hubble* exposures. The average number of satellite trails per typical exposure in would range from $5.9^{+0.6}_{-0.6}$ for SPHEREx, to more than 32^{+17}_{-13} in ARRAKIHS. At the lowest orbit altitude, *Xuntian* Space Telescope will be the most affected, with 86^{+20}_{-19} satellite trails per average exposure. One of every four exposures obtained with *Hubble* Space telescope will show contamination by satellite trails. The expected surface brightness of the Sun-illuminated satellite trails – confirmed by *Hubble* observations – range from $\mu = 16$ to 22 mag arcsec^{-2}, placing them orders of magnitude above the detectability limit.

In the Astro2020 Decadal Survey [28], the National Academy of Science states that *satellite constellations pose a parallel threat to the radio sky as to ground-based optical telescopes*. Expanding on this concern, the forecast presented here demonstrates that the threat is not limited to ground-based telescopes but extends to all LEO space telescopes. While analytical approximations can be obtained for certain orbits, the actual number of satellite trails may depend on mission-dependent factors including the survey design, exposure times, and the characteristics of the orbit of the observatory. In this paper, we estimate the number of satellite trails that cross the field of view of a set of observatories representing a range of orbital scenarios. This study complements similar tools created for ground-based telescopes [29, 30], and provides contamination level predictions for future and present space missions.

4.1 Future milestones and requirements

The International Astronomical Union Center for the Protection of the Dark and Quiet Sky[9] (February 2024) published a consolidated list of recommendations to satellite operators, manufacturers, and industry partners to minimize the impact of mega-constellations in astronomy[10]. These recommendations include 1) limiting the reflectivity of satellites, 2) minimize high-amplitude flares caused by orientation changes, 3) support an observing network to characterize the light contamination from satellites, and 4) perform bi-directional reflectance distribution function tests on the

[9] IAU CPS: https://cps.iau.org/
[10] CPS Consolidated recommendations: https://cps.iau.org/documents/44/Consolidated-CPS-Recommendations.pdf

surfaces of spacecraft, and share their properties with the astronomical community. In addition to these items, we emphasize the need for:

1. *Enabling prevention:* Identifying an optimal upper limit for the orbits of large satellite constellations, above which space telescopes can operate minimizing interference.
2. *Enabling avoidance:* Maintain an updated and historic open archive of live orbital solutions for each active and derelict spacecraft and potential debris associated with them, as well as equivalent cross sections and attitude angles.
3. *Enabling correction:* Higher precision orbital solutions. Orbital elements must be as precise as possible to enable prediction and avoidance of satellite trails. For reference, for the average *Hubble*–satellite distance in our simulations ($d_{\rm sat} = 1500$ km) the orbital solution must be precise up to 3.5 cm to identify the trail with a 0.05 arcsec resolution. In contrast, the precision of the widely used TLE orbit propagation format is one kilometer [31].

LEO space telescopes are sensitive to satellites not only above, but also below their orbit altitude, depending on the Earth limb avoidance angle. In fact, CHEOPS ($h = 700$ km) observations have already been affected by satellite trails from satellites located at ~ 540 km [32]. Nevertheless, satellite constellations at lower orbits interfere less with the operations of all types of telescopes, since they are shadowed by the Earth for a longer period of time, rendering them virtually invisible even if illuminated by the full Moon (see Sec. 2). Limiting the satellite constellations to orbits lower than those of space telescopes is a promising method to prevent interference with astronomy. However, other potential implications of lower orbit satellite constellations must be considered, though. For example, it has been observed that the continuous reentries of satellites increase the amount of aluminum oxide nanoparticles in Earth's stratosphere, potentially depleting the ozone layer as the number of satellite constellations increase [33], and generating atmospheric temperature anomalies up to 1.5°C [34]. Placing satellite mega-constellations at extremely low orbits would increase atmospheric drag and increase the rate at which the satellites would burn up in reentry. It is therefore critical to designate safe and limited orbit layers for a sustainable use of space.

The brightness, and therefore the detectability, of satellites strongly depends on the relative orientation of the satellites with respect to the observer and the Sun. *Starlink* satellite orientation following launch is in an "open-book" orientation, with major axis of the satellite parallel to the ground to minimize drag during thrusting and orbital rising[11]. This open-book orientation maximizes the observed reflective surface for ground-based observatories, making them brighter. Upon achieving nominal orbit – and as part of the mitigation measures already applied by the industry – the satellites switch to an orientation that is perpendicular to the ground ("shark-fin") to minimize solar reflection to ground-based observers. However, this orientation increases the cross-section from the point of view of a LEO space telescope. Due to the solar panels' Sun-facing orientation, a space telescope pointing away from the Sun can easily receive the reflected light from the solar-panels [32]. In addition, mitigation

[11] Starlink presentation on AAS 2021: https://aas.org/sites/default/files/2020-06/SpaceX%20for%20SIA%20AAS%20Astronomy%20Webinar%205.26.20.pdf

plans based on attitude control depend on the end-of-life operations. As satellites become non operational, they might lose attitude control, tumbling, and reaching angles where more light than originally intended reach the telescopes, increasing the complexity of the satellite trails, making their potential correction more challenging or even impossible. Detailed de-orbit plans and enforcement policies are critical.

We are witnessing the beginning of a new era of widespread industrial exploitation of LEO, with an expected 20 to 100-fold increase on the number of artificial satellites. Reminiscent of the first reports on the effects of human-emitted chlorofluorocarbons (CFCs) and their depleting effect for the ozone layer in Earth's stratosphere [35] that led to the Montreal Protocol in 1980s, efforts to quantify the effects of satellite mega-constellations are being outpaced by the industry. Our results demonstrate that contrary to the popular belief, space-telescopes are not immune to the light contamination reflected by artificial satellites. We predict that tens (SPHEREx, ARRAKIHS) to hundreds (*Xuntian*) of satellite trails will appear on astronomical images of LEO space telescopes if the announced satellite constellations become operational. We propose a series of mitigation measures that can be applied to prevent, avoid, and correct the unwanted effect of satellite trails in space telescopes, enabling a responsible use of the Low Earth Orbit for both science and industry.

Supplementary information. The *Hubble* WFC3/UVIS observations analyzed in Sec.2.2 can be accessed via the following Digital Object Identifier doi: 10.17909/ta6d-ws88.

Acknowledgements. This research made use of observations obtained with NASA/ESA Hubble Space Telescope and made available from the Mikulski Archive for Space Telescopes (MAST) at the Space Telescope Science Institute, which is operated by the Association of Universities for Research in Astronomy, Inc., under NASA contract NAS 5–26555. Thanks to Rocío Velasco Poblaciones for her careful review of this manuscript.

Declarations

4.2 Funding

Support for this work was provided by the National Aeronautics and Space Administration through *Hubble* Cycle 30 Award HST-AR-17041, administered by the Space Telescope Science Institute.

4.3 Conflict of interest/Competing interests

The authors declare no competing interests.

4.4 Ethics approval and consent to participate

Not applicable

4.5 Consent for publication

All authors have approved the manuscript and the required declarations by the journal, agreeing with its submission to *Nature*.

4.6 Data availability

4.7 Materials availability

4.8 Code availability

This work makes use of `Skyfield` [24], an open-source software to compute the positions for the stars, planets, and satellites in orbit around the Earth. `Skyfield`, and the analysis tools used in this work were programmed in `Python`.

4.9 Author contribution

A. B. led the analysis and writing of the paper. P. M. oversaw the project progress, assisted with the interpretation of the results and design of the analysis, preparation of the manuscript, and managed the funding to support the project. S. H. assisted with the interpretation of the results and the preparation of the manuscript.

5 Supplementary information

Table 1 Planned satellite mega-constellations (March 14, 2025)

Name	State	Version	Layers	Altitude	First launch	Launched	Planned
(1)	(2)	(3)	(4)	(5) [km]	(6) [year]	(7)	(8)
SferaCon	*Russia*		1	8070	2022	2	640
Telesat	*Canada*		3	1315 – 1335	–	–	300
OneWeb	*USA*	*P1*	2	1200	2019	660	716
		P2	3	1200	–	–	6372
HVNET	*USA*		1	1150	–	–	1440
Xingwang	*China*		5	860 – 1150	2021	36	966
Guangwang	*China*		7	508 – 1145	–	–	12,992
Hongyan	*China*		1	1100	2018	1	320
Hongyun	*China*		1	1075	2017	1	80
KLEO	*Denmark*		1	1050	2019	4	300
Ningxia	*China*		1	865	2019	10	50
SpinLaunch	*USA*		1	830	–	–	1190
Qianfan	*China*		1	806	2024	90	32
Bluewalker	*USA*		1	735	219	5	243
Astra	*USA*		6	380 – 700	–	–	13,620
Globalstar3	*Germany*		5	485 – 700	–	–	3080
SPHEREx (650 km)							
Cinnamon-937	*USA*		28	528 – 638	2022	4	337,323
Kuiper	*USA*		3	590 – 630	2023	2	3232
Starlink	*USA*	*G1*	5	488 – 570	2018	4714	6736
		G2.1	3	523 – 535	2022	3357	10,000
		G2.2	9	340 – 614	–	–	30,436
Semaphore	*France*		21	415 – 600	–	–	116,640
Starshield	*USA*		1	578	2022	138	32
Hubble Space Telescope (540 km)							
Honghu-3	*China*		6	340 – 550	–	–	10,000
Rassvet	*Russia*		1	550	2023	6	900
Yinhe	*China*		1	511	2020	8	1000
Lynk	*USA*		1	500	2020	10	2000
Hanwha	*China*		1	500	–	–	2000
Xuntian Space Telescope (CSST, 450 km)							
Total				340 – 8070	–	9048	562,640

Properties of present and future satellite telecommunication constellations. Col.(1) Name; Col.(2) Country; Col.(3) Constellation version; Col.(4) Number of satellite layers; Col.(5) Range (in km) of satellite orbital altitude; Col.(6) Year of first launch; Col.(7) Total number of satellites launched (as of March 14, 2025); Col.(8) Total number of satellites planned. Reference: Jonathan McDowell mega-constellation database: https://planet4589.org/index.html.

Table 2 Specification of Low Earth Orbit telescopes

Name	Operator	h	i	λ	Exp. time	FOV	Δx
(1)	(2) [year]	(3) [km]	(4) [degree]	(5) [μm]	(6) [s]	(7) [degree^2]	(8) [arcsec]
Hubble	NASA/ESA	540	28.47	$0.2 - 1.6$	540 ± 370	3.1×10^{-3}	0.05
SPHEREx	NASA	650	97	$0.7 - 5$	112.5	39.5	6.2
Xuntian	CSA	450	41.47	$0.2 - 1.7$	100 - 500	1.2	0.073
ARRAKIHS	ESA	650 - 800	TBD	$0.3 - 1.6$	600	1.4	~ 1.5

Properties of the considered space telescopes. Col.(1) Name; Col.(2) Operator; Col.(3) Launch date (* = planned); Col.(4) Telescope orbital altitude (in km); Col.(5) Telescope orbital inclination (in degrees); Col.(6) Spectral window of sensitivity (μm); Col.(7) Field of view (in degrees^2); Col.(8) Spatial resolution (in arcsec). Note: ARRAKIHS is a planned ESA F-class mission proposal. The parameters shown here represent published proposed configurations [19, 20] and they are subject to potential changes.

References

[1] Deshpande, A. A. & Lewis, B. M. Iridium satellite signals: A case study in interference characterization and mitigation for radio astronomy observations. *New A* **8**, 1940009 (2019).

[2] Falle, A., Wright, E., Boley, A. & Byers, M. One million (paper) satellites. *Science* **382**, 150–152 (2023).

[3] McDowell, J. C. The low earth orbit satellite population and impacts of the spacex starlink constellation. *ApJ* **892**, L36 (2020).

[4] Corbett, H. *et al.* Orbital foregrounds for ultra-short duration transients. *ApJ* **903**, L27 (2020).

[5] Grigg, D. *et al.* Detection of intended and unintended emissions from starlink satellites in the ska-low frequency range, at the ska-low site, with an ska-low station analogue. *A&A* **678**, L6 (2023).

[6] Ivezić, Ž. *et al.* Lsst: From science drivers to reference design and anticipated data products. *ApJ* **873**, 111 (2019).

[7] Hainaut, O. R. & Williams, A. P. Impact of satellite constellations on astronomical observations with eso telescopes in the visible and infrared domains. *A&A* **636**, A121 (2020).

[8] Tyson, J. A. *et al.* Mitigation of leo satellite brightness and trail effects on the rubin observatory lsst. *AJ* **160**, 226 (2020).

[9] Halferty, G., Reddy, V., Campbell, T., Battle, A. & Furfaro, R. Photometric characterization and trajectory accuracy of starlink satellites: implications for ground-based astronomical surveys. *MNRAS* **516**, 1502–1508 (2022).

[10] Mallama, A. The brightness of visorsat-design starlink satellites. 2101.00374 (2021).

[11] Mallama, A., Cole, R. E., Harrington, S. & Respler, J. Brightness Characterization for Starlink Direct-to-Cell Satellites. *arXiv e-prints* arXiv:2407.03092 (2024).

[12] Mallama, A., Cole, R. E., Tilley, S., Bassa, C. & Harrington, S. Bluewalker 3 satellite brightness characterized and modeled. arXiv:2305.00831 (2023).

[13] Williams, A., Hainaut, O., Otarola, A., Tan, G. H. & Rotola, G. Analysing the impact of satellite constellations and eso's role in supporting the astronomy community. *The Messenger* **184**, 3–7 (2021).

[14] Walker, C. *et al.* Impact of satellite constellations on optical astronomy and recommendations toward mitigations (2020).

[15] Kruk, S. *et al.* The impact of satellite trails on hubble space telescope observations. *Nature* **7**, 262–268 (2023).

[16] Feder, R. M. *et al.* The universe spherex will see: Empirically based galaxy simulations and redshift predictions. *ApJ* **972**, 68 (2024).

[17] Su, D.-Q. & Cui, X.-Q. Two suggested configurations for the chinese space telescope. *Afz* **14**, 1055–1060 (2014).

[18] Gong, Y. *et al.* Cosmology from the chinese space station optical survey (css-os). *ApJ* **883**, 203 (2019).

[19] Corral van Damme, C., Prod'Homme, T., Isaak, K., Rühl, T. & Sirianni, M. Coyle, L. E., Matsuura, S. & Perrin, M. D. (eds) *Arrakihs: Esa's new fast-implementation science mission.* (eds Coyle, L. E., Matsuura, S. & Perrin, M. D.) *Space Telescopes and Instrumentation 2024: Optical, Infrared, and Millimeter Wave*, Vol. 13092 of *Society of Photo-Optical Instrumentation Engineers (SPIE) Conference Series*, 130920Q (2024).

[20] Guzmán, R. *Arrakihs: The new esa f-class mission to investigate the nature of dark matter*, 1990 (2024).

[21] Wetzel, A. R. *et al.* Reconciling dwarf galaxies with Λcdm cosmology: Simulating a realistic population of satellites around a milky way-mass galaxy. *ApJ* **827**, L23 (2016).

[22] Drakos, N. E. *et al.* Deep realistic extragalactic model (dream) galaxy catalogs: Predictions for a roman ultra-deep field. *ApJ* **926**, 194 (2022).

[23] Crill, B. P. *et al.* Lystrup, M. & Perrin, M. D. (eds) *Spherex: Nasa's near-infrared spectrophotometric all-sky survey.* (eds Lystrup, M. & Perrin, M. D.)

Space Telescopes and Instrumentation 2020: Optical, Infrared, and Millimeter Wave, Vol. 11443 of *Society of Photo-Optical Instrumentation Engineers (SPIE) Conference Series*, 114430I (2020).

[24] Rhodes, B. Skyfield: High precision research-grade positions for planets and earth satellites generator (2019).

[25] Greynolds, A. W. Kahan, M. A. & Levine-West, M. B. (eds) *General physically-realistic brdf models for computing stray light from arbitrary isotropic surfaces.* (eds Kahan, M. A. & Levine-West, M. B.) *Optical Modeling and Performance Predictions VII*, Vol. 9577 of *Society of Photo-Optical Instrumentation Engineers (SPIE) Conference Series*, 95770A (2015).

[26] Lu, Y. Impact of starlink constellation on early lsst: a photometric analysis of satellite trails with brdf model. arXiv:2403.11118 (2024).

[27] Bassa, C. G., Hainaut, O. R. & Galadí-Enríquez, D. Analytical simulations of the effect of satellite constellations on optical and near-infrared observations. *A&A* **657**, A75 (2022).

[28] National Academies of Sciences Engineering, and Medicine. *Pathways to Discovery in Astronomy and Astrophysics for the 2020s* (2021).

[29] Lawler, S., Boley, A. & Rein, H. Visibility predictions for near-future satellite megaconstellations (2021).

[30] Osborn, J., Blacketer, L., Townson, M. J. & Farley, O. J. D. Astrosat: forecasting satellite transits for optical astronomical observations. *MNRAS* **509**, 1848–1853 (2022).

[31] Hartman, P. G. Long-term sgp4 performance. space control operations technical note. Tech. Rep., J3SOM-TN-93-01. US Space Command (1993).

[32] Billot, N. *et al.* In-situ observations of resident space objects with the cheops space telescope. arXiv:2411.18326 (2024).

[33] Ferreira, J. P., Huang, Z., Nomura, K.-i. & Wang, J. Potential ozone depletion from satellite demise during atmospheric reentry in the era of mega-constellations. *Geophys. Res. Lett.* **51**, e2024GL109280 (2024).

[34] Maloney, C. M., Portmann, R. W., Ross, M. N. & Rosenlof, K. H. Investigating the potential atmospheric accumulation and radiative impact of the coming increase in satellite reentry frequency. *New A* **130**, 2024JD042442 (2025).

[35] Molina, M. J. & Rowland, F. S. Stratospheric sink for chlorofluoromethanes: chlorine atomc-atalysed destruction of ozone. *Nature* **249**, 810–812 (1974).